Green light-emitting diodes used for stimulation of luminescence

R. B. Galloway and M. A. Neal

Department of Physics and Astronomy, The University of Edinburgh, Mayfield Road, Edinburgh EH9 3JZ, Scotland.

(Received 25 July 1997 ; in final form 10 February 1998)

This note concerns measurements of the spectra of the light emitted by diodes which have been used for the stimulation of luminescence from quartz. The measurements justify previous empirical conclusions concerning the choice of optical filters for separation of luminescence from scattered stimulating light. Also, past indirect inference of the optical power from the LEDs at the sample is substantiated by direct measurement. Data is presented on three LEDs, the III-V number TLMP7513 as used in the first account of the stimulation of luminescence by green LEDs (Galloway, 1992), the Toshiba TLPGA183P which was briefly investigated as as a possible improvement, and the recently produced Nichia NSPG-500 which has proved to be a substantial improvement on the original (Galloway *et al.*, 1997, in which the Nichia NSPG-500 was denoted 110104). The manufacturer's specifications for these diodes are summarised in table 1.

Optical spectra from one of each type of diode were measured using a spectrophotometer (type EO-85 made by Daedalon Corporation, 35 Congress Street, Salem, MA 01970, U.S.A.) which comprised a 25 μm wide slit from which light was collimated on a 700 lines/mm holographic grating, with the diffracted light focused by an f/1.8 50 mm lens on to a CCD detector of 1728 active pixels (with additional pixels for dark signal subtraction). A PC microcomputer displayed and recorded the spectral data. A spectrum from the type NSPG-500 LED at a current of 20 mA is shown in fig. 1. Of principal interest for luminescence stimulation are the wavelength at the maximum intensity and the range of wavelengths of light emitted. This information is summarised in table 1, in which the range of wavelengths of light emitted is indicated by the full width at half maximum and by the short and long wavelengths at which the intensity falls to 0.5% of the peak value. The 0.5% of peak intensity was the lowest intensity that could be distinguished from background noise, which can be seen in fig. 1 as the finite intensity recorded extending to the extremes of the wavelength scale.

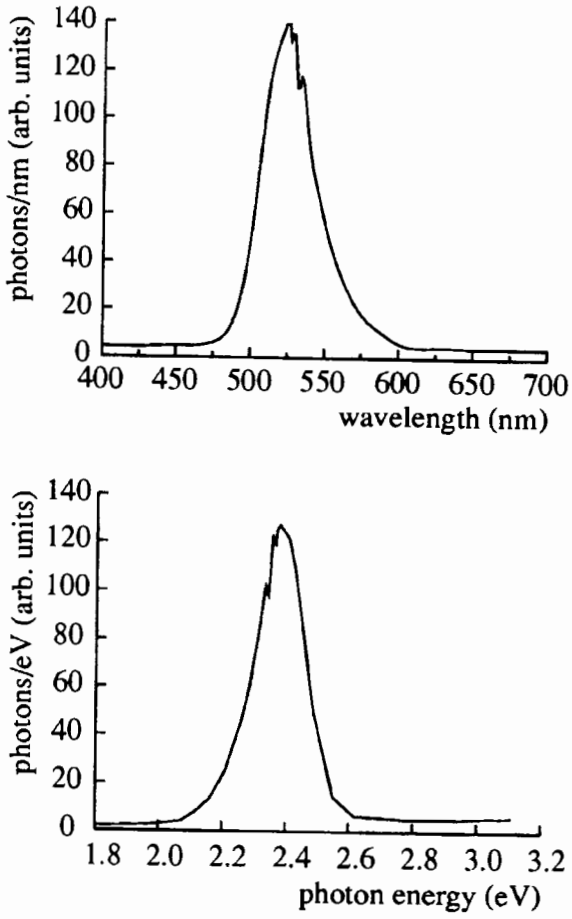

Figure 1.
A spectrum (corrected for the variation of sensitivity of the CCD with wavelength) from the Nichia NSPG-500 LED at a current of 20 mA with, for comparison, the spectrum plotted in terms of photon energy.

The emission spectrum is not symetrical; for diode type NSPG-500 (fig. 1) the fall in intensity from the peak towards shorter wavelengths is sharper than the

fall towards longer wavelengths; the same is true for diode type TLMP7513; the reverse is the case for diode type TLPGA183P, which has the sharpest emission peak.

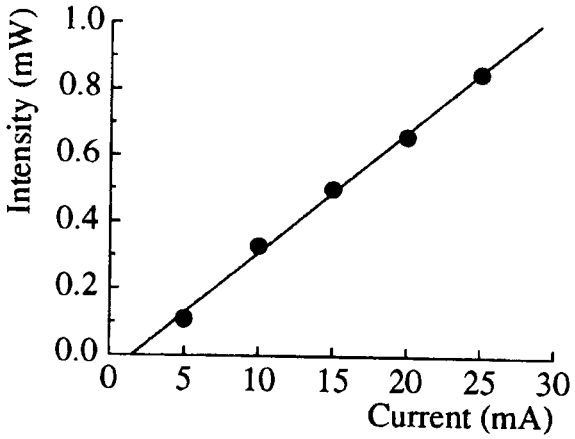

Figure 2.
The power emitted within a 20° cone by the NSPG-500 LED related to the current through the diode. The measurements were made using an optical power meter with pin diode, supplied by Ealing and factory calibrated at 652 nm.

For all three diodes the emitted light intensity is proportional to the current through the diode from 5 mA up to the maximum specified by the manufacturer (data for diode type NSPG-500 is shown in fig. 2), with no noticeable change in the shape of the spectrum. Further, there is no change in spectral shape with time from switching on the current through the diode. A current of 20 mA was switched through the diode under test and spectra recorded (which takes 140 ms measurement time) immediately and after 30, 60, 120, 240, 480 seconds. The only change with time since switch-on was that the initial spectrum showed a slightly higher intensity, of a few percent. This small change in intensity with time since switch on was investigated further by using a photomultiplier (type 9635QA) preceded by a neutral density filter to detect the change in photon counting rate with time, fig. 3. For the NSPG-500 diode, the photon counting rate during the first two seconds was 3% above the average value during the following 250 s. The (3 ± 0.6)% initial decrease in intensity is reproducible. The TLMP7513 diode showed a (6 ± 0.7)% initial decrease. The TLPGA183P diode was not tested in this way. Fig.3 shows that for the NSPG-500 diode, after the first two seconds the counting rate decreased by 1% in 4 minutes. Three similar measurements over a period of 2500 s indicated that, after the first 2 s, the counting rate increased by (1 ± 1)% in 40 minutes.

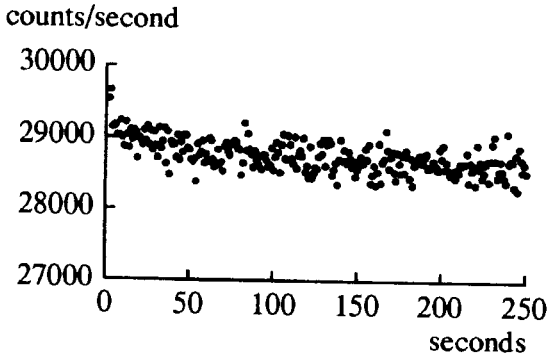

Figure 3.
The number of photons recorded in 250 successive 1 s intervals immediately following the switching of 20 mA through a Nichia type NSPG-500 LED, with the photomultiplier protected by a neutral density filter. The first two points are 3% above the mean. After the first 2 s, the decrease is 1% in the following 4 minutes.

Although it was not possible to follow the short wavelength side of the spectrum from the type NSPG-500 diode to less than 0.5% of the peak intensity, the fall from 50% to 0.5% was approximately exponential, and extrapolation to shorter wavelengths indicated that $\sim 10^{-4}$ of the total intensity could be emitted at wavelengths less than 400 nm. When using these diodes to stimulate quartz luminescence, the typical filter combinations used to separate luminescence from scattered green light transmit light of wavelengths less than 400 nm. The power output from the type NSPG-500 diode corresponds to the emission of 1.8×10^{18} photons/s, so that $\sim 10^{14}$ photons/s could be in the pass-band of the luminescence selecting filter. Even if this simple calculation is off by several orders of magnitude, the need to deal with it is clear. In line with these findings, it had been noted empirically (Galloway *et al.*, 1997) that Schott GG475 'long-pass' filters in front of the diodes adequately blocked the short wavelength photons when the type NSPG-500 were used for stimulation; without them the luminescence detecting system was swamped by scattered light.

The power emitted within a 20° cone by each LED was measured using an optical power meter with pin diode (supplied by Ealing Electro-Optics plc, Graycaine Road, Watford, Herts, WD2 3PW, U.K., factory calibrated at 652 nm), table 1. Thus the system of 16 type NSPG-500 diodes (Galloway *et al.*, 1997) should have about 11 mW illuminating the 1 cm^2 sample, in agreement with the indirect estimate of about

10 mW cm^{-2} made from the time taken to reduce luminescence from quartz to 50% of the initial value.

In changing from the type TLMP7513 diodes (Galloway, 1992) to the type NSPG-500 diodes (Galloway et *al.*, 1997) an improvement in efficiency of luminescence stimulation of 70 times was attributed to the change in diodes. This should be due in part to the increased power from the diodes (~14 times from table 1) and in part to the increased sensitivity of quartz to the shorter wavelength light. The sensitivity change on changing from 565 nm to 525 nm (2.20 to 2.37 eV) stimulation is 5 times (Huntley *et al.*, 1996; Botter-Jensen *et al.*, 1994; Spooner, 1994). Combining the diode power ratio and the sensitivity change gives a factor of 70 in agreement with the measured ratio ~70.

References

Botter-Jensen, L., Duller, G.A.T. and Poolton, N.R.J. (1994) Excitation and emission spectrometry of stimulated luminescence from quartz and feldspars. *Radiat. Meas.*, **23**, 613-616.

Galloway, R.B. (1992) Towards the use of green light emitting diodes for the optically stimulated luminescence dating of quartz and feldspar. *Meas. Sci. Technol.*, **3**. 330-335.

Galloway, R.B., Hong, D.G. and Napier, H.J. (1997) A substantially improved green-light-emitting diode system for luminescence stimulation. *Meas. Sci. Technol.*, **8**, 267-271.

Huntley, D.J., Short, M.A, and Dunphy, K. (1996) Deep traps in quartz and their use for optical dating. *Can. J. Phys.*, **74**, 81-91.

Spooner, N.A. (1994) On the optical dating signal from quartz. *Radiat. Meas.*, **23**, 593-600.

manufacturer	III-V	Toshiba	Nichia
type no.	TLMP7513	TLPGA183P	NSPG-500[(a)]
specification:			
peak wavelength (nm)	565	562	525
emission angle (deg.)	25	8	15
luminous intensity (mcd at 20 mA)	300	272-1288	3000-6000
max. current (mA)	25	50	30
measured (for 20 mA):			
peak wavelength (nm)	567 ± 2	570 ± 2	522-526 ± 2
FWHM (nm)	30 ± 2	11 ± 2	42 ± 2
0.5% of peak intensity (nm)	475 ± 20, 655 ± 10	510 ± 10, 620 ± 10	420 ± 10, 655 ± 10
power into 20° cone (mW)	0.051 ± 0.005	0.076 ± 0.005	0.687 ± 0.005

Note: (a) The Nichia NSPG-500 was denoted 110104 in Galloway et al. (1997), the part number used by our supplier, M.I. Cables Ltd., Inverness IV3 6EX, Scotland.

Table 1.
Properties of the light emitting diodes tested.

Reviewer
D.J. Huntley

Distinguishing burnt from partly bleached unburnt quartz pebbles of Pedra Furada, Brazil

Mostafa Michab, Hélène Valladas, Laurence Froget, and Norbert Mercier

Laboratoire des Sciences du Climat et de l'Environnement, Unité mixte CNRS-CEA, Avenue de la Terrasse, 91198 Gif sur Yvette Cedex, France.

(Received 16 March 1998 ; in final form 27 April 1998)

Abstract: D*iscussed in this article are the effects of light and heat on the TL emissions of quartz pebbles from Brazilian paleoindian site of Pedra Furada. The means used to distinguish specimens heated in prehistoric hearths and datable by TL from unheated and partly sunbleached will be discussed.*

Introduction

Excavations of the Upper Pleistocene prehistoric site of *Toca do Boqueirão do Sítio da Pedra Furada* (Piaui, Brazil) have uncovered a series of occupation levels radiocarbon dated to between 5,000 and over 48,000 years BP (Guidon and Delibrias, 1986; Guidon *et al*., 1994). Since the lower strata gave ages at the limit of C-14 dating it seemed advisable to try and date them by some other method. TL seemed appropriate since the ancient hearths at the site yielded transparent quartz pebbles showing such signs of past heating as surface reddening.

One of the problems encountered in trying to date them by TL was how to tell adequately heated dateable specimens from unheated ones that might have been partially sunbleached before burial, because preliminary measurements indicated that the traditional criteria whereby saturation of the TL signal is used to tell burnt quartz from unburnt were unsuitable for the quartz pebbles from Pedra Furada. The TL signal varied from sample to sample but increased in all instances after additional irradiation in the laboratory. Since these relatively translucent pebbles were protected from light after excavation one must assume that before being covered by sediment they remained exposed to sunlight for an unspecified period of time.

Effects of light exposure on quartz specimens

Numerous studies (Wintle, 1979; Aitken, 1985; Spooner *et al*., 1988; Smith *et al*., 1990; Zhou and Wintle, 1994; Feathers, 1997) have shown that when sedimentary quartz grains are exposed to sun light their TL is partially bleached. To see if the BPF pebbles have indeed been bleached, several randomly-selected quartz pebbles from the site were crushed, sieved, and the 100-160 μm fraction subjected to bleaching experiments. The TL was measured in our TL oven equipped with a Thorn EMI 9635QB photomultiplier and a 2 mm thick MTO UV filter with a maximum of transmission at 325 nm which allowed TL measurements up to 600°C (Valladas and Valladas, 1979); the heating rate was $10°s^{-1}$. The curves in all the figures of this article have been traced after the background emission has been substracted. Figures 1A-2A show the natural TL of samples BPF115 and BPF117 and the residual TL of the same two samples after they were exposed for varying periods of time (3, 6, 12, 24, and 30 hr) to a halogen lamp (OSRAM, HQI-T, 250 watt/D) placed 30 cm away. Figures 1B-2B show the relative decline of the peaks having maxima near 300, 400, and 500 - 600°C as a function of duration of exposure to light.

After about 5-10 hr of exposure the peaks in the vicinity of 300 and 400°C shrunk to about 10% of their original size and became practically undetectable after 20 hr. The 510°C peak of BPF115 took about 30 hr to decline to 10% of initial value, while after the same length of exposure the 550°C peak of BPF117 still retained about 80% of its value. After these samples were bleached the TL induced by artificial irradiation was similar in shape to the NTL (fig. 3). The other specimens exhibited similar behavior.

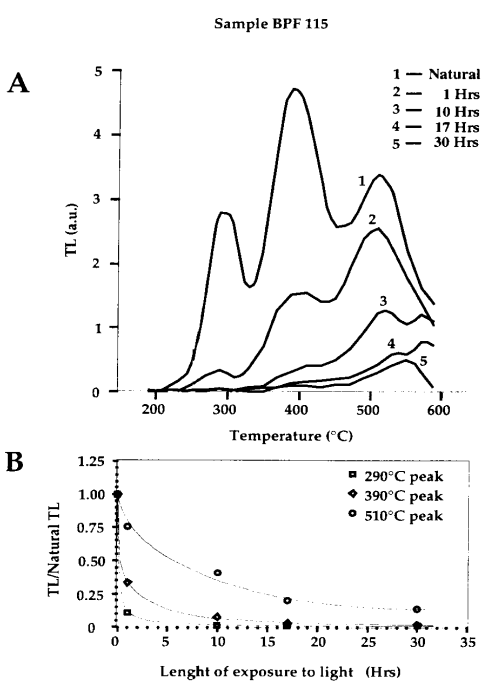

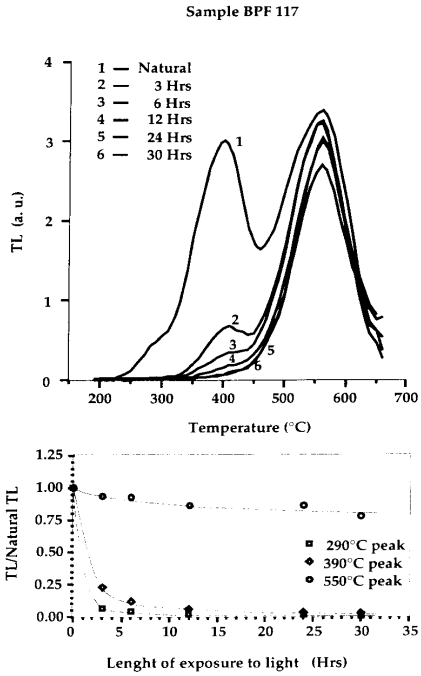

Figures 1 & 2.
Bleaching experiments on samples BPF115 (Figure 1), and 117 (Figure 2)
A - NTL and TL emissions obtained after different durations of light exposure varying between 1 to 30 hours.
B - Variation of the amplitude of the peaks near 300, 400, and 500-600°C as a function of length of exposure to light.

The results tend to strengthen our suspicion that TL emissions between 300 and 500°C of some of our quartz pebbles were probably partially bleached by exposure to sunlight before becoming covered by sediment. Unfortunately, such bleaching cannot be used to date unburnt pebbles by TL, since the residual TL is a function of opacity and pebble size, which in our work ranged from 100 to 800 g. Only specimens heated at 500°C or above were dateable, so it became paramount to establish viable criteria for recognizing such specimens.

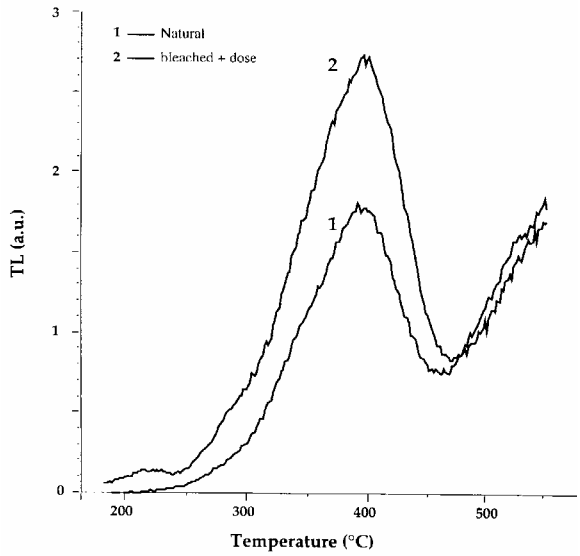

Figure 3.
Comparison of the NTL of sample BPF103 (curve 1) with the ATL (curve 2) obtained after this sample has been bleached and irradiated with a dose of 40 Gy.

The effects of heating on raw quartz pebbles

To see how the temperatures attained by such quartz pebbles might affect their TL properties, we collected six unburnt quartz pebbles at some distance from the Pedra Furada hearths and performed the following experiments on them.

1) The central core of each pebble was crushed, sieved, and the 100-160 µm grains saved.

2) Each powder sample was divided into five aliquots, which were placed in an electric furnace, heated at a rate of 25°C/min to a maximum of 200, 300, 400, 500, and 600°C, respectively, and allowed to cool slowly after staying at the peak temperature for 5 minutes. Each aliquot then received 40 Gy of gamma radiation from a ^{137}Cs source.

3) The natural (geological) and artificial TL of all six pebbles were measured using a MTO 380 nm optical filter which selected the blue component of the spectrum.

Some of the glow curves obtained for specimens BPF103, 78, and 71, are shown in Figures 4 and 5 (a-b). The geological TL of unheated pebbles, curve 1 in each figure, shows a maximum at about 400°C (heating rate : 5°s^{-1}). As one can see by comparing curves 1 and 2 in Fig. 4, the TL signal of quartz grains irradiated after being heated at temperatures inferior to 400°C has a shape similar to geological TL. The behavior of BPF103 is typical of the other similarly treated samples. When the heating temperature attains or exceeds 500°C the artificial TL signal (curve 3 in Fig. 4 and curve 2 in Fig. 5a or b) shows a 400°C peak accompanied by a new one at about 300°C. The sensitivity of the latter increases with temperature (curve 4 in Fig. 4 obtained after a 600°C heating), a phenomenon already noted by (David *et al*., 1977).

These experiments indicated that when Pedra Furada quartz is heated at 500°C and irradiated it exhibits TL peaks at 300 and 400°C. On the other hand, if the same sample is reheated at a temperature of 500°C, or lower, the TL obtained after same irradiation remains unchanged (Fig.6).

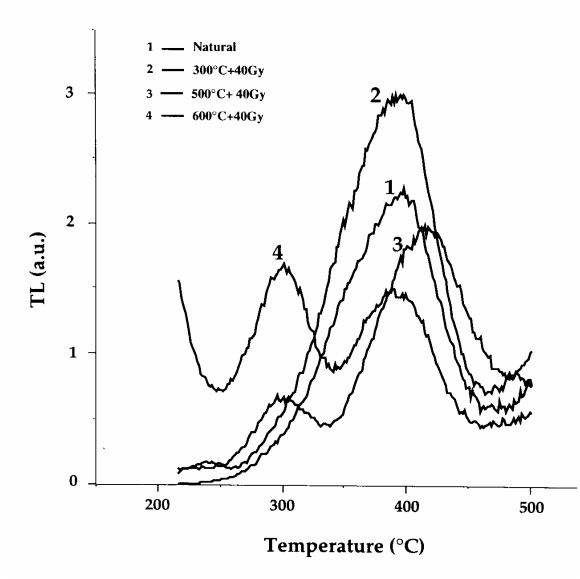

Figure 4.
Effect of heating temperature on the TL emission of the raw quartz pebble BPF103
Curves 1 ———> NTL (geological TL)
Curves 2, 3, and 4 ———> TL emissions obtained after this sample has been heated respectively at 300 (curve 2), 500 (curve 3) and 600°C (curve 4) and irradiated with an artificial dose of 40 Gy

Thus one can see that exposure to temperatures of 500°C or higher left an indelible mark on the TL signal of Pedra Furada quartz. The glow curves obtained after laboratory irradiation exhibited a distinct maximum near 300°C which was absent in curves of similarly treated but unheated specimens. The shape of the TL signal in the 300-400°C range allows one to select specimens that have been exposed to high enough temperatures to be dateable.

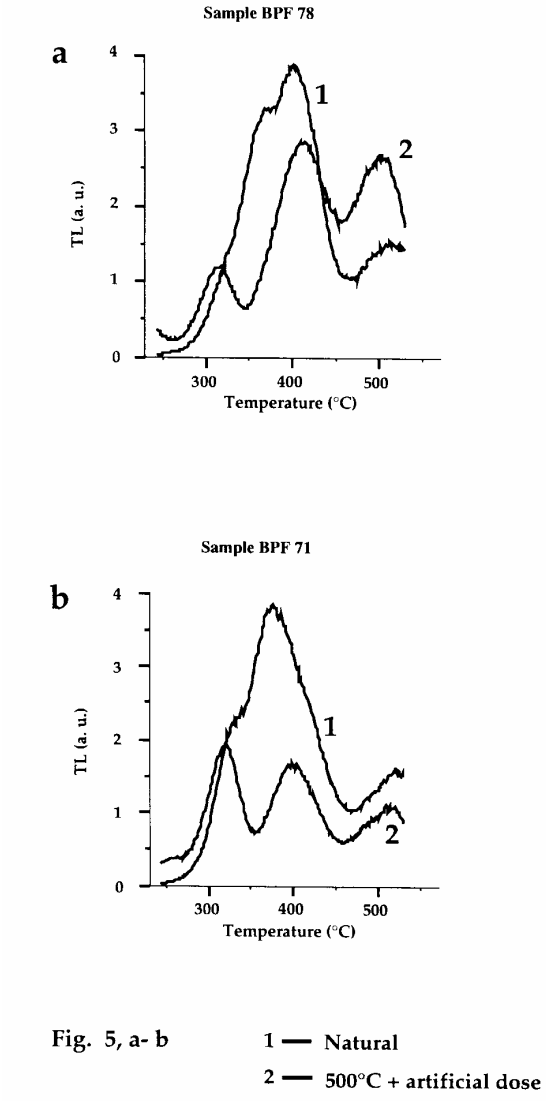

Figure 5.
Comparison between the geological TL of samples BPF78, and 71 and the TL glow curves obtained after these samples have been heated at 500°C and irradiated with an artificial dose of 40 Gy

How this criterion was used to select for dating sample BPF53, collected near a hearth, is shown by the data in Figure 7. Since the natural TL (curve 1) exhibits a distinct peak at about 300°C, in addition to the one near 400°C, the specimen must have been heated at a temperature no lower than 500°C and is consequently dateable. Moreover, as in the case of experimental sample BPF103 (Fig.6), one can see that after a second heating at 500°C followed by irradiation the glow curve of BPF53 remained unaltered (Fig. 7).

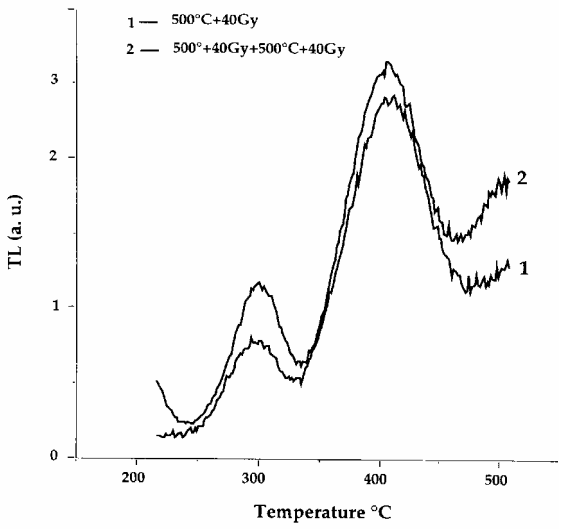

Figure 6.
Effect of two successive heatings at 500°C on the TL emission of sample BPF103

Curve 1 : TL emission induced by an artificial dose of 40 Gy obtained after the sample has been heated at 500°C

Curve 2 : TL emission induced by an artificial dose of 40 Gy obtained after the sample has been heated twice at 500°C

In Figure 8 are plotted the natural and natural + artificial TL of BPF50 for artificial doses of 30, 60, and 90 Gy. The paleodose was determined by the *Normalization Method* (Valladas and Gillot, 1978; Mercier *et al*., 1992) using the second TL growth curve (regeneration curve). The paleodose of 28±3 Gy was constant between 350 and 430°C (plateau test), so the specimen was suitable for dating.

The age estimates for the samples discussed above will be published after we have obtained all the relevant dosimetric data.

Acknowledgments
We wish to thank Georges Valladas and Jean Faïn for several useful comments.
Contribution No. 0056 from the Laboratoire des Sciences du Climat et de l'Environnement (LSCE), Gif sur Yvette.

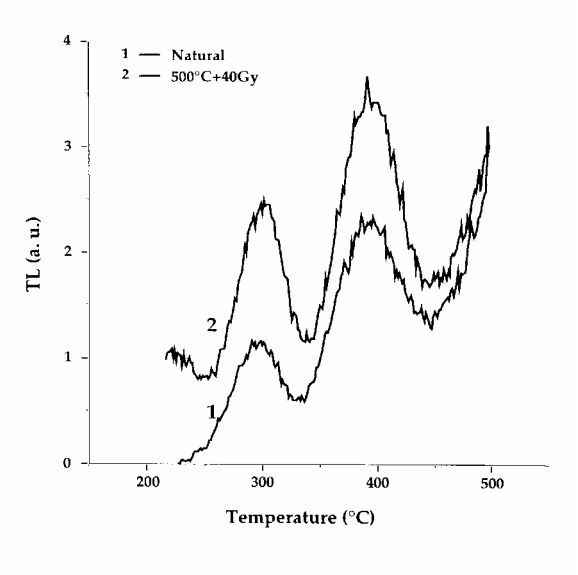

Figure 7.
NTL of sample BPF53 and TL emission induced by an artificial dose of 40 Gy after the sample has been heated at 500°C

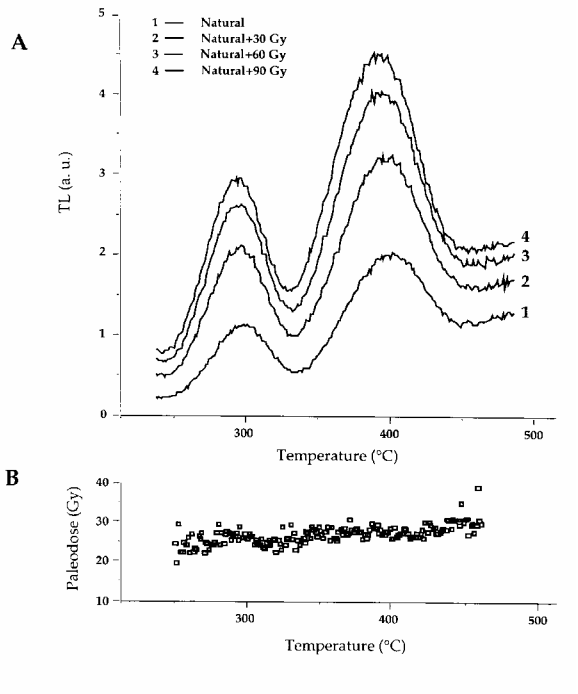

Figure 8.
Paleodose measurement on sample BPF50
A - NTL and artificial TL obtained after successive irradiations of 30, 60 and 90 Gy
B - Plateau test : Paleodose as a function of temperature

References

Aitken, M. J. (1985) *Thermoluminescence Dating.* Academic Press, London.

David, M., Sunta, C. M., and Ganguly, A. K. (1977) Thermoluminescence of quartz : part II. Sensitization by thermal treatment. *Indian J. Pure and Appl. Phys.* **15**, 277-280.

Feathers, J.K. (1997) Luminescence dating of sediment samples from white paintings rockshelter, Botswana. *Quaternary Geochronology (Quaternary Science Reviews)* **16**, 321-331.

Guidon, N., and Delibrias, G. (1986) Carbon - 14 dates point to man in the Americas 32,000 years ago. *Nature* **321**, 769-771.

Guidon, N., Parenti, F., Da Luz, M. d. F., Guérin, C., and Faure, M. (1994) Le plus anciens peuplement de l'Amérique : le Paléolithique du Nordeste brésilien. *Bulletin de la société préhistorique française* **91**, 246-250.

Mercier, N., Valladas, H., and Valladas, G. (1992) Some observations on paleodose determination in burnt flint. *Ancient TL* **10**, 28-32.

Smith, B. W., Rhodes, E. J., Stokes, S., Spooner, A., and Aitken, M. J. (1990) Optical dating of sediments : initial quartz results from Oxford. *Archaeometry* **32**, 19-31.

Spooner, N. A., Prescott, J. R., and Hutton, J. T. (1988) The Effect of Illumination Wavelength on the Bleaching of the Thermoluminescence (TL) of Quartz. *Quaternary Science Reviews* **7**, 325-329.

Valladas, G., and Gillot, P. Y. (1978) Dating of the Olby lava flow using heated quartz pebbles : some problems. *Pact* **2**, part one, 141-150.

Valladas, G., and Valladas, H. (1979) High temperature thermoluminescence. *Archaeo-Physika* **10**, 506-511.

Wintle, A. G. (1979) Thermoluminescence dating of sediments. *PACT* **3**, 374-380.

Zhou, L. P., and Wintle, A. G. (1994) Sensitivity change of thermoluminescence signals after laboratory optical bleaching: experiments with loess fine grains. *Quaternary Geochronology (Quaternary Science Reviews)* **13**, 457-463.

Reviewer
J. Faïn

Some methodological techniques for luminescence imaging using an IPD

C. J. McFee

Research Laboratory for Archaeology and the History of Art,
6 Keble Road,Oxford, UK.OX1 3QJ
(Present Address : Room 1016A, Building A2, Defence Evaluation and Research Agency, Farnborough, Hants GU14 0LX, UK.)

(Received 28 October 1997 ; in final form 6 May 1998)

Abstract: *An Imaging Photon Detector (IPD) can be used to obtain quantitative TL or IRSL images of the luminescence distribution in a mineral or pottery slice, or to measure the luminescence from individual mineral grains. Properties of the IPD itself, such as resolution and speed of response to the photon flux are important characteristics which will have important consequences for experimental design. However, the range of experiments that are possible in imaging studies are also dependent on the experimental system as a whole, such as the optics used, and the detector characteristics. In this paper the behaviour of such a system, using an IPD as the detector, is described, The consequences for the experimental methodologies adopted are also discussed, as are the range of measurements that are achievable from such a system.*

1. Introduction.

The lack of spatial discrimination of a photomultiplier (PM) tube denies the experimenter important information about the thermoluminescence (TL) or infra-red stimulated luminescence (IRSL) within a sample, whether it is a planchette containing many thousands of coarse-grains (90-180 μm) minerals, or a mineral or pottery slice. Only an integrated signal can be measured, and information on grain-to-grain or spatial variation in the luminescence is not available.

The obvious way of finding such information from single grains is by using a PM tube, picking and glowing out each grain individually (Miallier *et al.*, 1985, Grün *et al.*, 1989). However, the signal-to-noise ratio is often poor. To improve the signal to noise ratio larger grain sizes may be used. In addition, the photocathode can be physically or magnetically shielded from most of the thermal radiation from the heater plate, with only the photons originating from the area of the grain being measured (Wintle 1974, Sutton and Zimmerman, 1976). However, these measurements can be very time consuming and the need to illuminate the grains to be able to see them whilst picking can cause problems with IRSL measurements due to the highly light-sensitive nature of the IRSL traps (even if an image intensifier is used to view the grains whilst picking them). Recently, Bailiff *et al.* (pers. com.) have used a PM to detect the OSL signal stimulated by scanning a laser across a sample in a raster type scan pattern to build up an image of the OSL.

The problems associated with using a PM tube as the detector can be overcome using imaging detectors. Such techniques allow the luminescence distribution of mineral/pottery slices to be easily seen, and, if the luminescence distributions of individual grains are required, a large number of grains may be imaged in one measurement, saving a lot of time. However, it may be more difficult to obtain quantitative measurements using imaging techniques. In addition, the signal to noise ratio using imaging may not be as good as that obtained using a shielded PM tube or raster techniques.

Luminescence images may be found using photographic techniques, or by using a solid state imager. For example, Hashimoto *et al.* (1986, 1989), obtained TL colour images for a number of quartz samples and showed that it was possible to obtain quantitative TL information from these images. However, large (several kGy) doses had to be given to the quartz samples to maximise the TL counts. Huntley and Kirkey (1985) used an image intensifier to obtain the semi-quantitative distribution of the

natural TL from a quartz sample. An image intensifier was also used by Templer and Walton (1983) to study the TL from a number of zircon grains.

More recently, Duller *et al.* (1997) described a luminescence imaging system using a Charge Coupled Device (CCD) mounted on a Risø automated TL/OSL reader. This device enables quantitative luminescence images to be made at only a medium cost to the user. Integration effects limit the minimum time over which an image can be obtained (0.1s in this case). However, this is unlikely to be a major problem for the majority of measurements contemplated.

In this paper, the imaging techniques and methodologies adopted for luminescence imaging using an Imaging Photon Detector (IPD) are discussed. An IPD is a multichannel plate device which enables quantitative imaging of both TL (Smith *et al.* 1991, McFee and Tite 1998) and IRSL (McFee, forthcoming). The criteria adopted for selecting the optics which were eventually used with the IPD are described, followed by an examination of some of the potential problems which were found to be important in the optical arrangement used (and would lead to an incorrect measurement of the luminescence). Finally, two methodologies specifically adopted for imaging single grains are described and contrasted.

2. Maximising the resolution : the choice of optics.

An advantage of using a PM tube is that the tube is often placed directly above the sample to be measured. Thus, a large proportion of the available light is available to the photocathode. In contrast, in most imaging applications, optics will be required to focus the light onto the photocathode. This will reduce the overall aperture available for light collection. Therefore, great care needs to be taken when selecting suitable optics. For example, the optics initially used with the IPD were found to have a very poor resolution (Smith *et al.* 1991), with a 10mm aperture required to be placed in the optical path to remove any off-axis rays. However, this aperture heavily reduced the light throughput. Consequently, by considering the performance of the original optical system on the IPD, and by using a range of off the shelf lenses in a range of simple optical designs, a number of criteria were identified as being important in developing a new optical system for the IPD:

- the optics must be as aberration free as possible to allow the identification of individual coarse grains. Thus, grains would receive no additional light exposure above the minimum required for sample preparation and deposition;
- as large a depth of focus as possible is desirable as out of focus areas would lead to a significant loss of photons;
- a minimum working distance is necessary to accommodate a TL 'oven' (or an IRSL diode collar). With the oven used with the IPD, this distance was fixed at 15mm;
- a low magnification is usually desirable (<x10);
- as large a light gathering power and light throughput as possible is necessary to maximise the count rate.

The requirements above are difficult to satisfy in full. After considering a range of commercially available lenses it was decided that a reflecting objective, based on a Cassegrain system with a large primary mirror and a smaller secondary mirror, was the most appropriate lens. The advantages of this system were:

- zero chromatic aberration as there are no refracting optical elements (a problem with the previous lenses);
- a much longer working distance, for the same magnification, than with conventional refracting objectives;
- a large numerical aperture (0.5);
- wavelength range extends into the UV.

On the advice of an optical consultant, a suitable lens was purchased from Biorad, who manufacture microscope lenses for biological microscopes. The lens itself was an "off-the-shelf" lens, but had to be modified by the manufacturer to accommodate the working distance of 15mm.

Unfortunately, even after modification, the lens produced an image only 25mm above the housing of the lens, this was too short to project the image onto the photocathode of the IPD. Thus an additional 'relay' lens was required which produced a 1:1 image at the correct distance for the photocathode, the full optical set-up (i.e. reflecting objective and relay lens) is shown in figure 1. The secondary relay lenses were made of quartz with an effective transmission above 220nm, and were bought "off-the-shelf" from the Ealing Electro-optics catalogue. This final optical system was tested by visually imaging a series of test

bars in strong white light and the overall resolution of the system in white light was found to be better than 10μm with only small amounts of coma visible at the extremities of the field of view, no spherical aberration could be seen. The optical system was then tested by imaging a 180μm diameter pinhole at very low light levels (using a heavily filtered diode). These results are shown in table 1, together with the other specifications of the new and old optical systems.

	Original optics	New optics
Magnification of the optics	x 4	x 5.25
Best image size for the 120μm pinhole	600μm	180μm
Approximate depth of focus	n/a	300μm
Image field of view at the IPD Photo-cathode	25mm	19mm
Light Throughput (nominal values).	1 (with aperture)	14
Working distance of lens	n/a	25 mm
Effective object field of view	6.2mm	3.5mm

Table 1.
Measurements of the image size and depth of focus of the original optics, compared with the new values for the reflecting objective plus the secondary relay lens. The image sizes have been corrected for the magnification of the optics.

The resolution achieved with the new optics is more than sufficient to allow the imaging of either single grains or mineral/pottery slices, and the total light throughput of the optics has substantially improved. Although there has been a reduction in the image field of view, the grains can now be packed more closely together, due to the increased resolution. Consequently, the number of grains which can be imaged in a single measurement has not substantially declined.

The IPD is fitted with a bi-alkali photocathode, which is optimised towards the blue end of the spectrum. Although TL and IRSL measurements can be made with a range of filters, it was found that the use of blue sensitive filters (for example, a 7-59) limits the amount of light which falls onto the photocathode to the extent that, typically, only very bright grains can be seen. Consequently, the majority of measurements with the IPD were made using the broad-band BG39 filter. The transmission of the photocathode, combined with a BG39, is shown in figure 2.

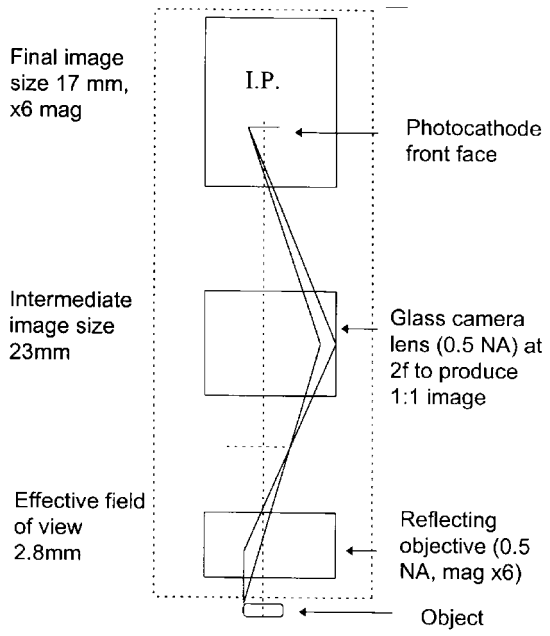

Figure 1.
The IPD optical setup

The light transmission of the IPD was compared with that of a "conventional" manual TL set (in which the PM tube is placed directly over the heating plate). The TL from a single coarse-grain of calcium fluoride was measured using both the "conventional" TL set, and the IPD). The IPD was found to be about 10 times less sensitive then this "conventional" set. The lower limit of detection for the IPD system varies, depending on grain size, sensitivity, etc. However, in general, most sediment samples were reasonably bright, and typically about half of the grains placed onto a planchette were visible when their natural TL was measured. In contrast, most pottery samples were very dim and only about 10 % at most were visible, even if the grains were given an appreciable radiation dose before glowing out. Similar results were found using IRSL. For typical sedimentary grains, about half of the grains which were placed onto the planchette had a measurable natural IRSL.

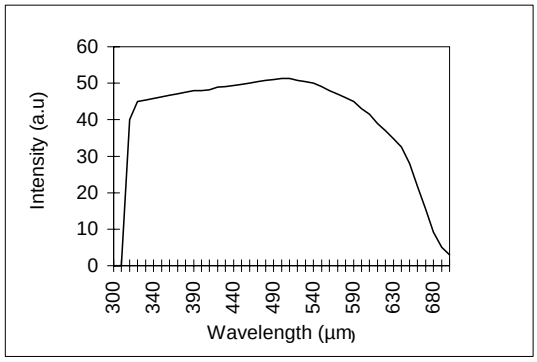

Figure 2.
The transmission of the quartz optics plus a BG39 optical filter.

3. Potential Problems from luminescence imaging.

Although a suitable optical system had been developed, a range of experimental factors needed to be addressed before an appropriate methodology could be defined. In particular, several major potential sources of error were identified as potentially leading to non-reproducible results when imaging mineral/pottery slices or single grains. These were:

- variation in transmission of the optics across the field of view;
- variation in photocathode sensitivity;
- variation in beta dose delivered to the slice/grains during an on-plate irradiation.

In addition, for single grains, changes in grain orientation between measurements may also lead to errors.

Each of these potential sources of error will be considered in turn.

3.1 Variation in transmission across the optics.

Figure 3 shows a flat field measurement across the IPD photocathode. It can be seen that the optics are not uniformly transmitting across the entire field of view. In addition, unless the IPD could be very accurately positioned above the sample, a small lateral displacement in position of the IPD or optics was found to lead to a large shift in image position on the photocathode. The causes of this shift in position are due to the current design of the IPD optical system. To allow samples to be placed onto the heater plate the entire IPD optical system (indicated by the dotted line in figure 1) can be raised and moved laterally to expose the heater plate. Although the IPD optical system was carefully constructed, it is not possible to re-place the IPD exactly in the same place with respect to the object on the heater plate. For example, a re-positioning of the IPD optical system of only 200µm displacement from the object will lead to an image displacement on the photocathode of over 1mm. Consequently, changes in the field of view of the optical system (see figure 3) could lead to substantial apparent differences in luminescence for otherwise identical measurements. However, a simple correction factor can be used to correct this observed luminescence, and a small calibration program was written to automatically assign a correction factor to any selected area, depending on its position within the field of view. Nevertheless, it is clear that, due to the rapid fall off in intensity near the edge of the field of view it is difficult to accurately apply a correction factor and large errors may be introduced. Thus, areas of interest near the periphery of the field of view were excluded from measurements to prevent erroneous measurements.

The sensitivity of the bialkali photocathode and the resistive anode will also vary with position and Smith *et al.* (1991) quote the variation from the IPD as ± 30%. However, for all measurements made here, any variation in the sensitivity of the IPD will have been included within the flat field correction made above.

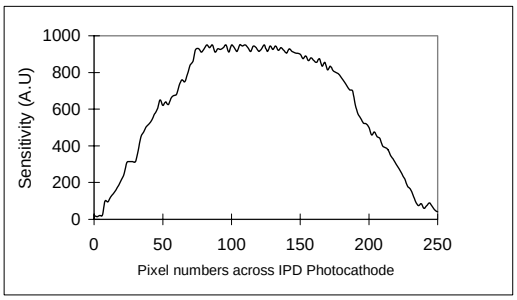

Figure 3.
A flat field measurement using the reflective objective and the secondary lens system. One pixel corresponds to approximately 0.1mm on the IPD photocathode.

3.2 Variation in beta dose across the sample during irradiation.

The beta dose rate delivered to a sample under laboratory irradiation will not be homogenous and there will be a diminution of the dose delivered at the extremities of a square planchette (10mm x 10mm). Aitken (1985, p123) quotes a difference of 10% in the dose between the centre and the extremes of a 10mm diameter stainless steel disc (for the seperation

of 2.5mm used here). However, the field of view of the new IPD optical system is less than 4mm. Thus, provided the sample is positioned correctly under the radiation source, it is likely that any differences in the beta dose rate across the field of interest will be insignificant compared to other possible sources of error discussed in this section. Consequently, they will be ignored.

3.3 Changes in grain orientation

The face which a grain presents to the photocathode will affect the total luminescence which can be measured. For example, Templer (1993) reported that the apparent TL sensitivity of a zircon grain could be altered by a factor of four, simply by turning a different face of the grain to the PM tube.

Possible errors due to changes in grain orientation were investigated by giving selected grains repeated cycles of a beta dose followed by a TL measurement, with each grain being viewed with a microscope between measurements, and then displaced with a needle to present a different face to the photocathode. In several cases the grains were physically removed altogether and then replaced. After every measurement, the TL from each grain was also corrected for any changes in position with respect to the field of view, as described in section 3.1 above. Several of the grains were specially selected because they had physical characteristics which it was thought would be most likely to show large variations in TL (for example, multi-faceted shapes or variable iron oxide staining on one face).

These measurements found that any variation in the TL due to the changes in grain orientation was no more than ±30% of the TL found in a single measurement.

In summary, several possible problems may occur in luminescence imaging. Variations in the beta dose in an irradiation applied to the area of interest were not considered important, whereas changes in grain orientation during a measurement could lead to errors in each measurement, but such errors are likely to be small (5-10%). The variations in transmission across the field of view, which could lead to large errors in the TL intensity measured in any single measurement, could be corrected for. However, this correction itself may also have a small error associated with it

Finally, as well as apparent differences in counts caused by a slight displacement of the image position on the photocathode, apparent changes in the TL could be found if small differences in the best focus postition occured, resulting in slightly different photon counts falling within an area of interest. Such differences would be particularly important when making measurements of the natural luminescence of single grains if inferences of, for example, the presence of any insufficiently bleached grains were made from these measurements .

The effect of each of these random variations is unlikely to be quantifiable. However, an empirical estimate of the total effect of such variations could be made by determining the range of TL intensities found from many grains after a repeated, identical measurement. Such an experiment is discussed below.

3.4 Measurement of the variation within a large number of grains

A large number of calcium fluoride grains were placed on a planchette. They were heated to 450 °C to zero the TL and were given a known laboratory beta dose. The grains were then glowed to 450 °C with a reheat to measure the blackbody radiation (glow 1). The grains were then given the same beta dose and glowed again (glow 2). The ratio of TL for glow 1/glow 2 were corrected for any positional differences for each grain within the field of view, as described in section 3.1. The ratios of glow1/glow2 are shown in figure 4 (a) and (b).

From this experiment, it can be seen that the TL intensities obtained from repeated, identical measurements may vary by up to a factor of four times (figure 4 (a)) if no correction for variation of grain position within the image field of view is applied. Applying the correction factor used in figure 3 reduces the largest difference in TL intensities obtained to 1.2 (figure 4 (b)).

The effect of applying a correction can be particularly seen for grains 180-200 where a large number of grains have a high ratio of glow1/glow2, presumably caused by a large movement of the image of the planchette within the field of view between measurements. This is greatly reduced after the correction has been applied.

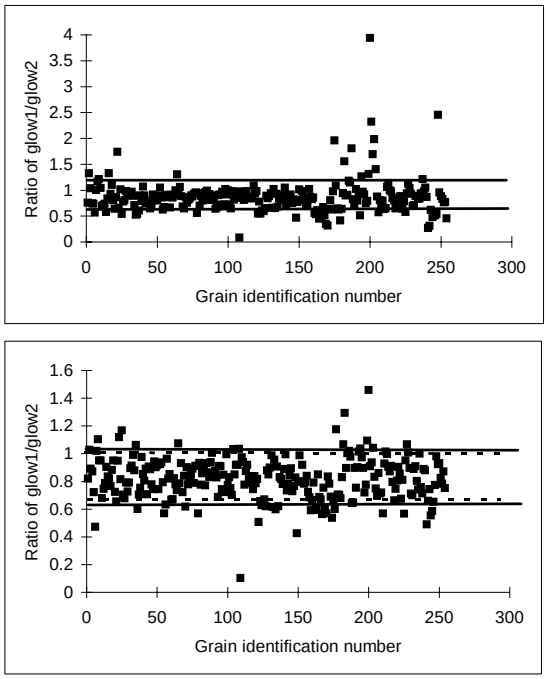

Figure 4.
(a, above) : The variation in the ratio of glow1/glow2 for 252 calcium fluoride grains; the TL measurements have not been corrected for changes in grain position due to planchette movement. The 1 sigma variation is shown
(b, below) : The same grains, but with a correction applied. The solid lines show the grains within ± 25% of the mean. The hatched lines show the 1 sigma variation. Note the changed scale.

The mean ratio for the grains without correction is 0.86 ±0.33 and with correction it is 0.82 ±0.15. The difference from the expected value of 1 is probably due to an increase in the TL sensitivity after the first TL measurement as the grains had no annealing treatment, before the zeroing of the TL by glowing to 450°C.

Figure 4 (b) also has plotted the 1σ standard deviation about the mean, and an arbitrarily chosen position which corresponds to ±25% around the mean value. When no correction is applied to the grains 187 out of 256 (73%) fall within ±25% of the mean, when a correction is applied it is 221 out of 256 (86%).

Therefore, the importance of correcting for differing planchette positions within the field of view is shown by figure 4. Applying a correction reduces the 1 sigma standard deviation by half, more importantly it corrects many potential outliers which would otherwise have large values of glow1/glow2.

However, despite this position correction the ratios of glow1/glow2 for all these grains do not share the same value. Although, after correction the number of grains falling in the ±25% band has increased, the variation in measurement values within this ±25% band appears quite similar. Most of the grains have been little affected by the correction for variation in planchette position, some not at all.

This experiment defined the minimum possible measurement reproducibility currently available from the IPD, which for the majority of measurements made was consequently taken as ±25%. This reproducibility is important because it points to the range of experiments that the IPD is very useful for, and conversely, those areas for which the IPD is not so suitable, these experiments are discussed further in section 5.

4. Methodologies adopted for imaging single grains

Although this paper has mainly concentrated on imaging single grains, the problems and solutions are just as valid for imaging mineral or pottery slices. However, for measuring single grains, one of two slightly different additional methodologies were adopted, the choice of methodology adopted depending on whether grains need to be physically identified after measurement, or if minimising the potential bleaching of any luminescence is more important. Both these methodologies will be discussed in turn.

method 1

Grains are hand picked with a small needle under subdued red light, using an image intensifier attached to a binocular microscope. The grains are then transferred onto a rhodium plated planchette which has small recesses drilled onto it to make a regular pattern (figure 5) to aid identification. The grains are not placed within the recesses but are grouped around the surface of the planchette surrounding each recess. It was found that placing a grain in a recess led to apparent differences in the TL intensities due to differences in reflectivity between the recess and the rest of the planchette. The TL image observed on the IPD is compared with the pattern seen when the planchette is examined with a microscope in reflected white light, after TL measurement.

Advantages of this method are:

- grains can be positively identified, allowing further investigations with, for example, a binocular microscope or an analytical SEM.

Disadvantages are:

- the considerable time needed to physically pick the grains and place them onto a rhodium planchette. As well as being very tedious, the grains will also be exposed to the subdued red light for an amount of time which could be sufficient to cause significant bleaching of samples, particularly if IRSL measurements are made;
- a limited number of grains may be imaged on each planchette.

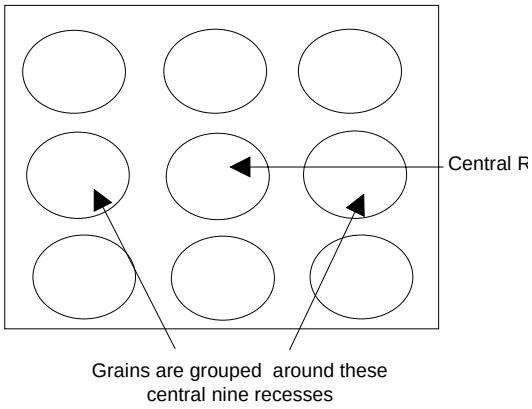

Figure 5.
The central portions of the rhodium plated planchette which are imaged by the IPD.

method 2

In this method the grains are not individually picked out but are prepared identically to the method adopted for preparing conventional stainless steel discs used for TL. A number of well-resolved grains may be selected from the TL image of the planchette.

Advantages of this method are:

- ease of preparation so that grains can be quickly prepared for measurement resulting in a saving of time and minimising possible bleaching;
- ability to measure more grains on a single planchette than in method 1.

Disadvantages of this method are:

- as the grains are randomly placed onto the planchettes some of them may be touching and consequently their images on the IPD cannot be completely resolved if there are insufficient counts to provide an adequate contrast between these grains. The data from these grains should be discarded;
- it is not possible to physically identify each grain after a TL measurement.

5. Conclusions

This paper has discussed some of the pitfalls that can occur in luminescence imaging, and the techniques adopted to try and overcome them. It is likely that some problems discussed in this paper are fundamental to luminescence imaging. For example, if single grains are to be measured, it is inevitable that the grains will have to be exposed to some light, unless the grains can be directly deposited on a disc and then resolved during the measurement.

However, it must be stressed that individual systems will have different problems associated with them. For example, an optical system with a larger field of view, or a system with less movement of the entire system between measurements, would not suffer the problems discussed in this paper to such an extent.

A careful assessment of the potential errors which could occur must be determined for individual systems, and this will determine to some extent the types of measurements that can be carried out with the system. For example, the IPD discussed in this paper was suitable for making measurements where very good reproducibility between measurements was not required. Thus, measurements of natural/second glow ratios to determine grains very bright in the natural TL were possible, as were diagnostic images of grains or pottery/mineral slices such as images of quartz using IRSL to investigate the possibility of feldspar inclusions within the grains (McFee, 1995).

However, when a good (within a few percent) measurement-to-measurement reproducibility is required, the IPD discussed in this paper is not so useful. For example, attempts to obtain single grain IRSL EDs proved only partially successful, using a weighted average it was possible to obtain an ED for a small number of grains that agreed with the ED found for the 'bulk' sample ED. However, the precision was such that it was not possible to distinguish between individual grain EDs (although a very high ED grain would still be clearly recognisable) (McFee, in press). Similarly, determination of fading rates for single grains was not possible with the system as it currently stands.

In summary, whilst luminescence imaging enables a wide range of measurements to be made, it is important to understand and characterise the behaviour of each individual system used. In addition, trade-offs within the choice of system used itself will also affect the type of measurements which are possible.

Acknowledgements

This work would not have been possible without the help of Adrian Allsop, Dave Seely and Martin Franks. Thanks to Lindsey Shepherd for help and comments on this paper.

References

Aitken, M.J. (1985) *Thermoluminescence dating*. Academic Press. London

Duller, G.A.T., Bøtter-Jensen, L., and Markey, B.G. (1997) A luminescence imaging system based on a charge coupled device (CCD) camera. *Radiation Measurements*, **27**, 91-99.

Grün, R., Packman, S.C., and Pye, K. (1989) Problems involved in TL-dating of Danish Cover Sands using K-feldspar. Long and Short Range Limits in Luminescence Dating, RLAHA Occasional Publication **9**.

Hashimoto, T., Koyanagi, A., Yokosaka, K., Hayashi, Y., and Sotobayashi, T. (1986) Thermoluminescence color images from quartzes of beach sands. *Geochemical Journal*. **20** , 111-118.

Hashimoto, T., Yokosaka, K., Habuki, H., and Hayashi, Y. (1989) Provenance search of dune sands using thermoluminescence colour images (TLCIs) from quartz grains. *Nucl. Tracks Radiat. Meas*., **16**, (1), 3-10.

Huntley, D.J., and Kirkey, J.J. (1985) The use of an image intensifier to study the TL intenstity variability of individual grains.*Ancient TL*. **3**(2) 1-4.

Miallier, D., Fain, J., and Sanzelle, S. (1985) Single grain quartz TL dating : an approach for complex materials. *Nucl. Tracks Radiat. Meas.*, **9**, 163-168.

McFee, C.J (1995) The Use of an Imaging Photon Detector for Luminescence Imaging Unpublished D.Phil thesis, University of Oxford.

McFee, C.J., (in press) The measurement of single grain IRSL EDs using an imaging photon detector. Accepted for publication in *Quaternary Geochronology*.

McFee, C.J., and Tite, M.S.. (1998) The detection of insufficiently bleached grains using an imaging photon detector. *Archaeometry* **40** (1), 153-168

Smith, B.W., Wheeler, G.C.W.S., Rhodes, E.J., and Spooner, N.A. (1991) Luminescence dating of zircon using an imaging photon detector. *Nucl. Tracks. Radiat. Meas*. **19**, 273-278.

Templer, R.H. (1993) Autoregenerative thermo-luminescence dating using zircon inclusions. *Archaeometry*, **35** (1), 117-136

Templer, R.H., and Walton, A.J. (1983) Image intensifier studies of TL in zircons. *PACT* **9**, 300-308.

Wintle, A.G. (1974) Factors determining the thermoluminescence of chronologically significant materials. Unpublished D.Phil. thesis, University of Oxford.

Sutton, S. R. and Zimmerman, D. W. (1976) Thermoluminescent dating using zircon grains from archaeological ceramics. *Archaeometry*, **18**, 125-134.

Reviewer :

H. Schwarcz

Single-aliquot and single-grain optical dating confirm thermoluminescence age estimates at Malakunanja II rock shelter in northern Australia

Richard Roberts[1], Hiroyuki Yoshida[1], Rex Galbraith[2], Geoff Laslett[3], Rhys Jones[4] and Mike Smith[5]

[1] Department of Earth Sciences, La Trobe University, Melbourne, VIC 3083, Australia
[2] Department of Statistical Science, University College London, London WC1E 6BT, UK
[3] CSIRO Mathematical and Information Sciences, Melbourne, VIC 3168, Australia
[4] Department of Archaeology and Natural History, Research School of Pacific and Asian Studies, Australian National University, Canberra, ACT 0200, Australia
[5] People and Environment Section, National Museum of Australia, Canberra, ACT 2601, Australia

(Received 3 May 1998 ; in final form 22 May 1998)

Introduction

The earliest direct ages for human occupation of Australia are 50–60 ka from Malakunanja II and Nauwalabila I rock shelters in the Northern Territory (Roberts, 1997). These ages were obtained from unheated quartz sediments using thermoluminescence (TL) dating at Malakunanja II (Roberts *et al.*, 1990a, 1990b) and optical dating at Nauwalabila I (Roberts *et al.*, 1994). At both sites, a combination of additive-dose and regenerative-dose multiple-aliquot procedures was used to estimate the palaeodoses, while the dose rates were determined principally from high-resolution gamma-ray spectrometry analyses (which showed that a condition of secular equilibrium presently exists in the ^{238}U and ^{232}Th chains).

The reliability of TL dating methods for some rock shelter deposits has since been thrown into doubt by TL ages of more than 100 ka reported for human occupation of the Jinmium site in north-western Australia (Fullagar *et al.*, 1996). It has been suggested, however, that the high TL ages at Jinmium are the result of insufficient exposure to sunlight of some grains before burial (Roberts, 1997; Spooner, 1998). This suggestion has now been confirmed by optical dating of individual quartz grains and by ^{14}C dating of charcoal fragments, the conclusion being that the entire deposit was formed in the last 10 ka (Roberts *et al.*, 1998).

We have now examined quartz grains from two key samples (KTL162 and KTL164) from Malakunanja II (Figure 1) and found that single-grain optical ages, multiple-grain optical ages, and TL ages agree at this site, thereby confirming the original age estimates.

Sampling and dating procedures

Sample KTL162 was collected from the same level as the lowest artefact and produced a TL age of 61 ± 10 ka. Sample KTL164 was taken from the level immediately overlying a small pit containing artefacts and gave a TL age of 45 ± 7 ka. Details of site stratigraphy, sample preparation, TL dating methods, and dose rate determinations have been published previously (Roberts *et al.*, 1990a, 1990b). In the original study, the random and systematic age uncertainties were summed arithmetically; here they are added in quadrature, following standard practice (Aitken, 1985: Appendix B).

The optical dating apparatus, methods and statistical models employed here follow those used in the Jinmium study (Roberts *et al.*, 1998). Palaeodoses were estimated using a single-aliquot regenerative-dose protocol, in which sensitivity is monitored by measuring the optically stimulated luminescence (OSL) induced by a small test dose applied after measuring each of the natural and regenerated OSL signals (Murray and Roberts, 1998; Murray and Mejdahl, submitted). The palaeodoses were divided by the published dose rates (0.77 ± 0.09 Gy ka^{-1} for

KTL162, and 0.91 ± 0.08 Gy ka^{-1} for KTL164; Roberts *et al.*, 1990a) to obtain the optical ages.

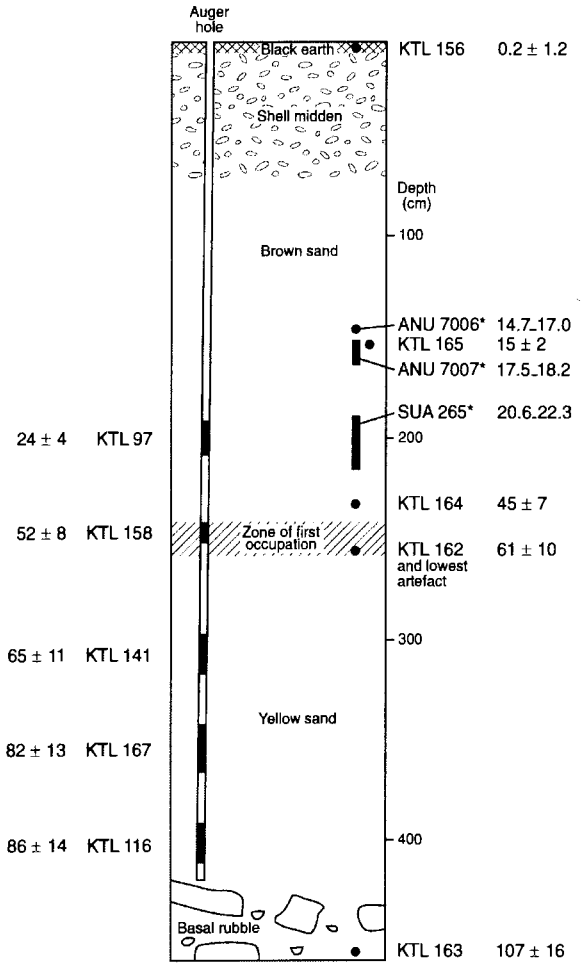

Figure 1.
Stratigraphic section of the Malakunanja II excavation (south-west face), showing the locations, depth intervals, and ages (in thousands of years) of the TL and ^{14}C samples. The three ^{14}C samples are marked by an asterisk. TL ages are given as mean age ± 1σ total uncertainty, while the calibrated (Stuiver and Reimer, 1993) ^{14}C ages are shown as 2σ age ranges.

Single-aliquot measurements

Optical dating was first applied to 24 aliquots of sample KTL162 and 24 aliquots of sample KTL164, with each aliquot being composed of many (~800) quartz grains of 90–125 μm diameter (the size fraction used also in the TL study). The dose (palaeodose) received by the mineral grains since their last exposure to sunlight was estimated for each aliquot using a range of preheat temperatures (160–300°C for 10s), test doses of 0.5 Gy, and a regenerative dose of 47 Gy (KTL162) or 42 Gy (KTL164).

Palaeodoses were constant with preheat temperature for both KTL162 (Figure 2) and KTL164, which we interpret as indicating negligible thermal transfer (except from traps responsible for the 110°C TL peak). The average palaeodose (for all 24 aliquots) was calculated for KTL162 (46.7 ± 1.2 Gy) and for KTL164 (41.5 ± 1.0 Gy), and these yielded ages of 60.7 ± 7.5 ka and 45.7 ± 4.1 ka, respectively.

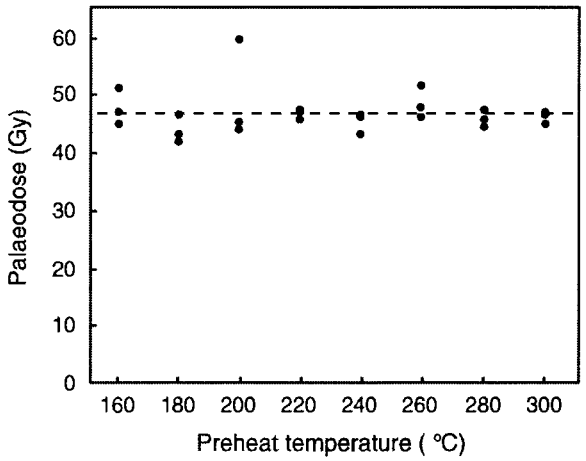

Figure 2.
Palaeodoses obtained from 24 aliquots of sample KTL162 at different preheat temperatures using a regenerative-dose protocol. Three aliquots were held for 10 s at each preheat temperature. Each aliquot was composed of ~800 grains and was stimulated for 100 s at 125°C. The uncertainty in palaeodose estimation (1σ level) for each aliquot is smaller than the size of the symbol. The plateau from 160°C to 300°C implies negligible thermal transfer, except from traps responsible for the 110°C TL peak (Murray and Roberts, 1998). The average palaeodose is marked by the dashed line.

Single-grain measurements

Palaeodoses were then estimated for 85 and 86 individual grains from KTL162 and KTL164, respectively, using a preheat of 270°C (KTL162) or 260°C (KTL164) for 10 s, test doses of 1 Gy, and a regenerative dose of 47 Gy (KTL162) or 42 Gy (KTL164). Palaeodoses were calculated using the measured natural, regenerative dose, and test dose OSL signals specific to each grain. The test dose signals were measured for each grain to correct for any change in sensitivity between the natural and regenerative dose cycles. Consequently, grains with

weak test dose signals yielded palaeodoses with correspondingly large relative errors.

Most of the 85 grains from KTL162 have palaeodoses of 30–50 Gy and none have significantly larger palaeodoses (the latter might indicate the presence of insufficiently bleached grains). One grain has a significantly smaller palaeodose (~16 Gy) and this grain is presumed to have intruded from the overlying deposits. Most grains were weakly luminescent and only 18 of them produced significant test dose signals (i.e. where the rate of luminescence decay during the first few seconds of optical stimulation was statistically greater than zero at the 2σ level). Figure 3(a) is a radial plot (see 'Discussion') of the palaeodoses determined for these 18 grains; the numerical values are given in the Appendix, together with the sensitivity changes monitored using the test dose signals.

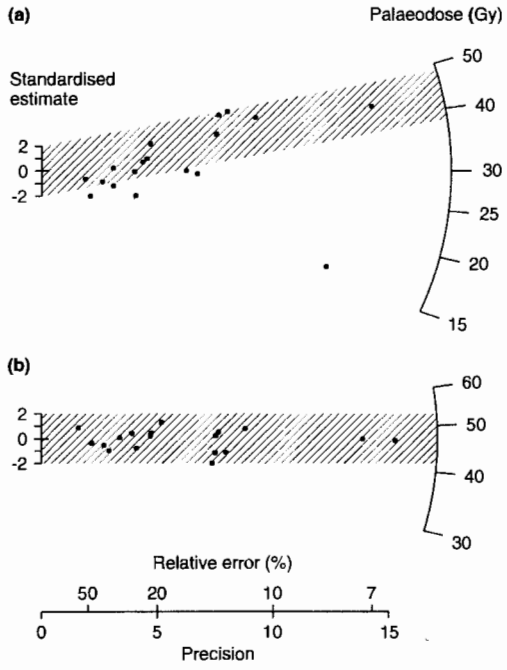

Figure 3.
(a) *Radial plot of palaeodoses determined for 18 individual grains (those with statistically significant test dose signals) from sample KTL162 using a regenerative-dose single-aliquot optical dating protocol. Single grains vary in luminescence intensity, resulting in differing palaeodose precisions. The y-axis plots standardised estimates of log palaeodose, given by log palaeodose minus a central value (log 30 Gy in this example), divided by the standard error of log palaeodose. The x-axis (precision) plots reciprocal standard errors of log palaeodose; these may be converted to approximate relative errors of palaeodose, which are also shown. Points on any straight line radiating from the origin have the same log palaeodose; a circular scale has been added so that palaeodoses (log scale) may be read off. For grains with the same true log palaeodose, 95% of the points should lie within ± 2 units (on the y-axis) of a common radial line, as shown by the hatched component centered at 42.7 Gy which corresponds to the estimate of central palaeodose (see 'Discussion'). Further details on radial plots are given by Galbraith (1988, 1990, 1994).*

(b) *Radial plot of the doses calculated for the same 18 individual grains plotted in (a) after bleaching each grain with 420–550 nm light (for 125 s at 125°C) and then giving a laboratory beta dose of 47 Gy to each grain. The hatched component is centered at the applied dose of 47 Gy and it can be seen that all points are statistically concordant with this dose.*

Each of the 85 grains from KTL162 was then given a second regenerative dose and a third test dose, and the regenerative-dose protocol was run again: the correct (known) dose was obtained for all grains, as illustrated in Figure 3(b) for the 18 grains with statistically significant test dose signals. This figure shows that all points are consistent with the applied dose of 47 Gy, taking into account their measurement errors. This experimental check is reassuring, although it does not account for heterogeneity in the beta dose rate that may occur in a field context and that could introduce an additional source of variation to the palaeodose values calculated for single grains buried at the same time.

Sample KTL164 showed a similar pattern of single-grain palaeodoses: most of the 86 grains have palaeodoses of 30–50 Gy, none have significantly larger palaeodoses, and one grain has a significantly smaller palaeodose (~19 Gy). The general consistency of palaeodose estimates for single grains from samples KTL162 and KTL164 implies a lack of significant post-depositional disturbance of the Malakunanja II sediments, indicating that artefacts are unlikely to have intruded into these levels.

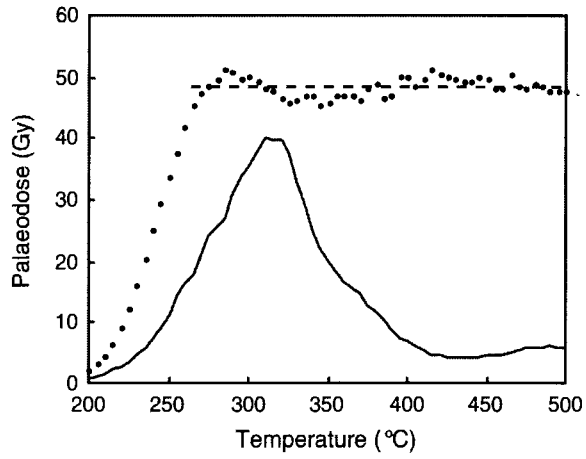

Figure 4.
TL palaeodose versus temperature plot for sample KTL162. Palaeodoses were determined by the total-bleach method (see Roberts et al., 1990a for experimental details). Palaeodose uncertainties (1σ level) are typically ± 10% or better, and the average palaeodose (~48 Gy) across the plateau region (270–500°C) is marked by the dashed line. The solid line shows the TL glow curve for a natural aliquot. Roberts et al. (1990a) present similar data for sample KTL164.

Discussion

A radial plot (Galbraith, 1988, 1990, 1994), rather than a histogram, has been used to plot single-grain palaeodoses because the precisions associated with palaeodose measurements differ considerably between grains due to their varying luminescence intensities. It is not appropriate to plot such palaeodoses on a histogram because a histogram takes no account of their varying precisions, and the inclusion of relatively imprecise points could seriously distort the frequency distribution. However, a histogram may be used to display points that have similar and high precisions, such as the palaeodoses calculated for single aliquots composed of multiple grains.

Application of a central-age model (modified from Galbraith and Laslett, 1993) to grains from KTL162 with high-precision palaeodoses (those with relative errors of ± 20% or better, excluding the ~16 Gy grain) gives a central palaeodose of 42.7 ± 3.6 Gy and an age of 55.5 ± 8.2 ka. Each estimate is quoted with ± 1 standard error, which represents the usual 68% confidence interval. A similar procedure applied to KTL164 (to the 12 grains with high-precision palaeodoses, excluding the ~19 Gy grain) yields a central palaeodose of 40.2 ± 2.3 Gy and an age of 44.2 ± 4.7 ka. The central palaeodose is an estimate of the geometric mean of the true (i.e. in the absence of measurement error) single-grain palaeodoses.

An additional parameter of interest is the dispersion of single-grain palaeodose populations. This parameter measures the relative standard deviation of the palaeodoses in the absence of measurement errors, so it indicates dispersion over and above the measurement error associated with each grain (following Galbraith and Laslett, 1993). In Figure 3(b), for example, all points are consistent with a common palaeodose of 47 Gy and the dispersion parameter is estimated to be zero.

For each of the two samples KTL162 and KTL164 (those grains with high-precision palaeodoses, excluding the ~16 Gy and ~19 Gy grains), the dispersion parameter is estimated to be ~17%. The relative standard deviation of the measured palaeodoses will be higher and will differ between grains, because each has an associated measurement error, and is about 18–26% for these samples. This estimate is similar in magnitude to the empirical relative standard deviation of 21–27% reported for the single-grain palaeodoses at Allen's Cave (Murray and Roberts, 1997). But all of these estimates of dispersion are somewhat uncertain because they are based on small numbers of grains.

Heterogeneity in beta dosimetry was considered to be the most likely explanation for the palaeodose dispersion at Allen's Cave (Murray and Roberts, 1997) because the deposit contains a mixture of quartz sand, carbonate, and aeolian silt and clay with strongly contrasting beta dose rates (Olley *et al.*, 1997). The Malakunanja II deposit, however, is composed of siliceous sands that are apt to exhibit much less variation in beta microdosimetry. We might therefore expect the Malakunanja II samples to have smaller palaeodose dispersions than the Allen's Cave sample, but further data are needed to permit a definitive comparison.

We are also further investigating the issue of post-depositional disturbance by selecting grains of larger diameter (200–2,000 μm) to profit from three potential advantages. First, larger grains may be less easily displaced by ground water percolation and by the small-scale activities of soil fauna, thereby minimising the number of intrusive grains encountered at any level within the deposit. Second, if luminescence intensity is approximately proportional to grain volume then 200–2,000 μm-diameter grains

should be 10–10,000 times brighter than 100 μm-diameter grains, so that appreciable test dose signals are produced by a greater proportion of individual grains. And third, the beta contribution to the total dose rate will be reduced for larger grains because of significant beta attenuation, and this should produce a correspondingly reduced dispersion in single-grain palaeodoses when the dispersion is caused by variations in beta microdosimetry.

Conclusions

These single-aliquot and single-grain optical dating results support our earlier TL-based findings that people were present in Australia at 50–60 ka. They also show that correct burial ages can be obtained using TL methods, provided the sediments are bleached sufficiently before burial to reset the dating signal. The Jinmium sediments failed to meet this requirement (Roberts, 1997; Spooner, 1998), whereas adequate bleaching at Malakunanja II is indicated by the modern TL age for the near-surface sample (Figure 1), the similarity of palaeodoses obtained from TL signals (at 325°C and 375°C) with markedly different susceptibilities to light (Figure 4), and the concordance of TL and ^{14}C ages at this site (Figure 1). Optical dating of single grains also provides a means of testing for significant post-depositional disturbance of rock shelter sediments.

Acknowledgements

We thank Jon Olley and Martin Aitken for comments on a draft on this manuscript. CSIRO Mathematical and Information Sciences kindly supported R.G. in Australia, and R.R. is supported by a Queen Elizabeth II Fellowship from the Australian Research Council.

References

Aitken, M.J. (1985). *Thermoluminescence Dating*. Academic Press, London.

Fullagar, R.L.K., Price, D.M. and Head, L.M. (1996). Early human occupation of northern Australia: archaeology and thermoluminescence dating of Jinmium rock-shelter, Northern Territory. *Antiquity* **70**, 751-773.

Galbraith, R.F. (1988). Graphical display of estimates having differing standard errors. *Technometrics* **30**, 271-281.

Galbraith, R.F. (1990). The radial plot: graphical assessment of spread in ages. *Nuclear Tracks and Radiation Measurements* **17**, 207-214.

Galbraith, R.F. (1994). Some applications of radial plots. *Journal of the American Statistical Association* **89**, 1232-1242.

Galbraith, R.F. and Laslett, G.M. (1993). Statistical models for mixed fission track ages. *Radiation Measurements* **21**, 459-470.

Murray, A.S. and Mejdahl, V. (submitted). Comparison of regenerative-dose single-aliquot and multiple-aliquot (SARA) protocols using heated quartz from archaeological sites. *Quaternary Science Reviews* (submitted).

Murray, A.S. and Roberts, R.G. (1997). Determining the burial time of single grains of quartz using optically stimulated luminescence. *Earth and Planetary Science Letters* **152**, 163-180.

Murray, A.S. and Roberts, R.G. (1998). Measurement of the equivalent dose in quartz using a regenerative-dose single-aliquot protocol. *Radiation Measurements* (in press).

Olley, J.M., Roberts, R.G. and Murray, A.S. (1997). Disequilibria in the uranium decay series in sedimentary deposits at Allen's Cave, Nullarbor Plain, Australia: implications for dose rate determinations. *Radiation Measurements* **27**, 433-443.

Roberts, R.G. (1997). Luminescence dating in archaeology: from origins to optical. *Radiation Measurements* **27**, 819-892.

Roberts, R.G., Jones, R. and Smith, M.A. (1990a). Thermoluminescence dating of a 50,000 year-old human occupation site in northern Australia. *Nature* **345**, 153-156.

Roberts, R.G., Jones, R. and Smith, M.A. (1990b). Stratigraphy and statistics at Malakunanja II: reply to Hiscock. *Archaeology in Oceania* **25**, 125-129.

Roberts, R.G., Jones, R., Spooner, N.A., Head, M.J., Murray, A.S. and Smith, M.A. (1994). The human colonisation of Australia: optical dates of 53,000 and 60,000 years bracket human arrival at Deaf Adder Gorge, Northern Territory. *Quaternary Science Reviews* **13**, 575-583.

Roberts, R., Bird, M., Olley, J., Galbraith, R., Lawson, E., Laslett, G., Yoshida, H., Jones, R., Fullagar, R., Jacobsen, G. and Hua, Q. (1998). Optical and radiocarbon dating at Jinmium rock shelter in northern Australia. *Nature* **393**, 358-362.

Spooner, N.A. (1998). Human occupation at Jinmium, northern Australia: 116,000 years ago or much less? *Antiquity* **72**, 173-178.

Stuiver, M. and Reimer, P.J. (1993). Extended ^{14}C data base and revised CALIB 3.0 ^{14}C age calibration program. *Radiocarbon* **35**, 215-230.

Appendix

Numerical values for the 18 individual grains from sample KTL162 that gave statistically significant test dose signals (see 'Single-grain measurements'). Columns 2 to 4 list the palaeodoses and 1σ uncertainties, as plotted in Figure 3(a). Columns 5 to 7 list the ratios and 1σ uncertainties of the regenerative/natural test dose signals.

Grain number	Palaeodose (Gy)	Standard error (Gy)	Relative error (%)	Test R / Test N	Standard error (Gy)	Relative error (%)
5	32.4	10.6	33	0.89	0.29	32
19	30.1	4.8	16	0.96	0.15	16
22	53.8	7.1	13	1.14	0.15	13
25	54.3	6.8	13	1.19	0.15	12
28	29.7	7.4	25	1.05	0.26	25
30	21.5	8.3	39	1.29	0.49	38
34	20.4	6.7	33	1.14	0.36	31
35	21.3	11.4	54	0.45	0.24	54
50	29.0	4.3	15	1.12	0.16	15
54	18.4	4.6	25	1.06	0.26	24
62	11.4	5.5	48	0.93	0.44	47
67	35.4	8.2	23	0.72	0.16	23
70	16.0	1.3	8	1.36	0.11	8
99	47.6	5.2	11	0.76	0.08	11
105	44.2	5.9	13	1.10	0.14	13
107	43.1	3.0	7	0.91	0.06	7
109	37.4	8.3	22	0.96	0.21	22
110	47.8	10.3	21	1.14	0.24	21

Reviewer

M.J. Aitken

Thesis Abstract

Thesis title : New Applications of Thermo-luminescence: Dating of Paleoseismic Events and Pedogenic Carbonates

Author : Debabrata Banerjee

Submitted to : The Gujarat University, India, under the supervision of Prof. A.K. Singhvi, for the degree of Doctor of Philosophy, september 1996.

The present thesis aimed at the development of luminescence techniques for providing a chronology of important geological processes, viz., paleoseismic events and carbonate formation periods.

1. Dating of Paleoseismic Events

A luminescence method for dating fault gouges was devised for the first time. The method assumes that faulting resets the geologically acquired luminescence of the fault gouge. This assumption was tested in various experiments. Studies on the dependence of luminescence age with the size of the gouge grain suggested that a plateau in luminescence ages below a certain critical grain size is a good indicator of complete resetting of the luminescence signal. Observation of substantially higher host rock paleodoses in comparison to fault gouges also suggests efficient resetting of luminescence during faulting. After the feasibility studies, fault gouges were collected from various Himalayan faults, viz., Nainital Fault, Sleepy Hollow Fault, Mohand Thrust and the Main Boundary Thrust. The luminescence analyses suggest the occurrence of neotectonic activity at the Nainital Fault and the Sleepy Hollow Fault at 41 ± 8 ka and 36 ± 5 ka. The Mohand Thrust was active at 59 ± 10 ka ago while tectonism is indicated along the Main Boundary Thrust (Nainital region) at 70 ± 12 ka. The luminescence ages are consistent with available ^{14}C formation ages of lakes created by faulting in these regions.

A second approach to date seismic events was the development of optical dating of seismites (overbank river/lake sediments deformed by earthquakes soon after deposition). This method assumes that the seismites have insignificant accumulated luminescence at the time of the earthquake. Seismites were collected from a modem seismically active site, Sumdo Valley, Himachal Pradesh, India. The luminescence ages of these seismites imply that seismic events occurred in Sumdo at ~ 90 ka, 61 ka, 37 ka and 26 ka.

2. Dating of Pedogenic Carbonates

The first practical luminescence method to date carbonates utilized changes in the dose-rate to mineral grains during their formation. The age of the carbonate is evaluated by dividing the difference of paleodoses to the mineral grain from the ambient sand and carbonate by the difference between the sand and carbonate alpha and beta dose-rates. The new method is less susceptible to post-depositional changes compared to ^{14}C and U-series disequilibrium methods. Carbonates were sampled from various sites in Thar Desert across an east-west transact of ~ 300 km. Luminescence ages are observed to be stratigraphically consistent and indicate that carbonate formation took place in Thar at ~ 100 ka, ~17 ka and ~ 2 ka. The carbonate formation periods suggested by the luminescence chronology were consistent with the epochs implied by local paleoclimatic data.

Notices

International Union for Quaternaire Research (INQUA)
Commission on Tephrochronology and Volcanism

International Union of Prehistoric and Protohistoric Sciences (IUSPP)
Commission 31: Humans and Active Volcanoes during Prehistory and Protohistory

Symposium Inter-INQUA and Inter-IUSPP
Tephrochronology and coexistence Humans-volcanoes

Le Puy-en-Velay, France

24-29 August 1998

Call for papers

Scientific programme
Oral presentations, exhibitions of posters and trips will be organised around the main topics:
-Late Ice Age global volcanism,
-the inter-relationship between tephrostratigraphy and archaeology in Quaternary stratigraphies,
-Hominids, adapting strategies in active volcanic areas

Other topics will include:
-regional tephrostratigraphic studies,
-dating techniques in tephrochronology and archaeology,
-impact of volcanism on climate,
-characterisation techniques of tephras,
-tephrostratigraphy and multidisciplinary researches
and other related topics

Languages
Official languages are English and French

Trips
Local trips will be organised to the principal Quaternary volcanic areas of Massif Central

Fees, accomodation
The conference fees are +1000FF (500FF for students) ; accomodation is partially free for persons presenting a communication.

Informations, registration :
Michel Léger
Syndicat Mixte de la Haute-Vallée de la Loire et du Mézenc
Mairie, 43370 Solignac-sur-Loire, France
Tel. : 33 4 71 03 11 46 Fax : 33 4 71 03 12 77 e-mail : loirmez@cs-conseil.fr

Introduction to Optical Dating

by M. J. Aitken

will be published by Oxford University Press in August: price £75 (hardback). Credit card orders can be placed by e-mail (<book.orders@oup.co.uk>) or fax (+44 (0) 1536 454518);
otherwise by post to CWO, OUP,Saxon Way West, Corby, Northants NN18 9ES,
UK. Post & package: free in UK, otherwise +10%.

Bibliography

The bibliography is compiled by **Ann Wintle**, using visits to the library, reprints sent by colleagues, the BIDS (Bath Information and Data Services) and GEOREF electronic data bases.

Arkhipov S.A. (1998) Stratigraphy and paleogeography of the Sartan glaciation in West Siberia. Quaternary International 45/46, 29-42.

Batchelor J.D., Symes S.J.K., Benoit P.H. and Sears D.W.G. (1997) Constraints on the thermal and mixing history of lunar surface materials and comparisons with basaltic meteorites. Journal of Geophysical Research - Planets 102 E8, 19321-19334.

Blümel W.D., Eitel B. and Lang A. (1998) Dunes in southeastern Namibia: evidence for Holocene environmental changes in the southwestern Kalahari based on thermoluminescence data. Palaeogeography, Palaeoclimatology, Palaeoecology 138, 139-149.

Chawla S., Gundu Rao T.K. and Singhvi A.K. (1998) Quartz thermoluminescence: dose and dose rate effects and their implications. Radiation Measurements 29, 53-63.

Christiansen H.H. (1998) Periglacial sediments in an Eemian-Weichselian succession at Emmerlev Klev, southwestern Jutland, Denmark. Palaeogeography, Palaeoclimatology
Palaeoecology 138, 245-258.

Cini Castagnoli J., Bonino G., Della Monica P. and Taricco C. (1997) Record of thermoluminescence in sea sediments in the last millennia. Il Nuovo Cimento 20C, 1-8.

Correcher V., Muniz J.L. and Gomez Ros J.M. (1998) Dose dependence and fading effect of the thermoluminescence signals in gamma- irradiated paprika. Journal of the Science of Food and Agriculture 76, 149-155.

Ding Y.Z. and Lai K.W. (1997) Neotectonic fault activity in Hong Kong: evidence from seismic events and thermoluminescence dating of fault gouge. Journal of the Geological Society, London 154, 1001-1007.

Engin B. and Guven O. (1997) Thermoluminescence dating of Denizili travertines from the southwestern part of Turkey. Applied Radiation and Isotopes 48, 1257-1264.

Feathers J.K. and Rhode D. (1998) Luminescence dating of protohistoric pottery from the Great Basin. Geoarchaeology 13, 287-308.

Felix C. and Singhvi A.K. (1997) Study of non-linear luminescence-dose growth curves for the estimation of paleodose in luminescence dating: results of Monte Carlo Simulations. Radiation Measurements 27, 599-609.

Franklin A.D. (1997) On the interaction between the rapidly and slowly bleaching peaks in the TL glow curves of quartz. Journal of Luminescence 75, 71-76.

Frechen M., Horvath E. and Gabris G. (1997) Geochronology of Middle and Upper Pleistocene loess sections in Hungary. Quaternary Research 48, 291-312.

Fuller I.C., Macklin M.G., Lewin J., Passmore D.G. and Wintle A.G. (1998) River response to high-frequency climate oscillations in southern Europe over the past 200 ky. Geology 26, 275-278.

Göksu H.Y., Stoneham D., Bailiff I.K. and Adamiec G. (1998) A new technique in retrospective dosimetry: pre-dose effect in the 230°C TL glow peak of porcelain. Applied Radiation and Isotopes 49, 99-104.

Gorton N.T., Walker G. and Burley S.D. (1997) Experimental analysis of the composite blue cathodoluminescence emission in quartz. Journal of Luminescence 72-74, 669-671.

Götze J. and Magnus M. (1997) Quantitative determination of mineral abundance in geological samples using combined cathodoluminescence microscopy and image analysis. European Journal of Mineralogy 9, 1207-1215.

Halperin A. (1997) The nature of the electron traps in quartz associated with the thermoluminescence (TL) peaks in the range 70-700K. Annales de Chimie-Science des Materiaux 22, 595-600.

Hashimoto T., Sugai N., Sakaue H., Yasuda K. and Shirai N. (1997) Thermoluminescence (TL) spectra from quartz grains using on-line TL-spectrometric system. Geochemical Journal 31, 189-201.

Hubner S. and Göksu H.Y. (1997) Retrospective dosimetry using the OSL-pre-dose effect in porcelain. Applied Radiation and Isotopes 48, 1231-1235.

Jacobi R.M., Rowe P.J., Gilmour M.A., Grun R. and Atkinson T.C. (1998) Radiometric dating of the Middle Palaeolithic tool industry and associated fauna of Pin Hole Cave, Creswell Crags, England. Journal of Quaternary Science 13, 29-42.

Juyal N., Singhvi A.K. and Glennie K.W. (1998). Chronology and paleoenvironmental significance of Quaternary desert sediment in southeastern Arabia. Quaternary Deserts and Climatic Change. Rotterdam, Balkema. 315-325.

Kar A., Felix C., Rajaguru S.N. and Singhvi A.K. (1998) Late Holocene growth and mobility of a transverse dune in the Thar Desert. Journal of Arid Environments 38, 175-185.

Liritzis I. (1994) Archaeometry: dating the past. Ekistics 368/369, 361-366.

Liritzis I. and Bakopoulos Y. (1997) Functional behaviour of solar bleached thermoluminescence in calcites. Nuclear Instruments and Methods B 132, 87-92.

Liritzis I., Galloway R.B. and Hong D.G. (1997) Single aliquot dating of ceramics by green light stimulation of luminescence from quartz. Nuclear Instruments and Methods in Physics Research B 132, 457-467.

Liritzis I., Guibert P., Foti F. and Schvoerer M. (1997) The Temple of Apollo (Delphi) strengthens novel thermoluminescence dating method. Geoarchaeology 12, 479-496.

Little T.A., Grapes R. and Berger G.W. (1998) Late Quaternary strike slip on the eastern part of the Awatere fault, South Island, New Zealand. Geological Society of America Bulletin 110, 127-148.

Martini M. and Meinardi F. (1997) Thermally stimulated luminescence: new perspectives in the study of defects in solids. Rivista del Nuovo Cimento 20, 1-71.

McFee C.J. and Tite M.S. (1998) Luminescence dating of sediments - the detection of high equivalent dose grains using an imaging photon detector. Archaeometry 40, 153-168.

Michel V., Falgueres C. and Dolo J.M. (1998) ESR signal behavior study at g ~ 2.222 of modern and fossil bones for heating palaeotemperature assessment. Radiation Measurements 29, 95-103.

Murray A.S. and Roberts R.G. (1997) Determining the burial time of single grains of quartz using optically stimulated luminescence. Earth and Planetary Science Letters 152, 163-180.

Murray A.S. and Wintle A.G. (1998) Factors controlling the shape of the OSL decay curve in quartz. Radiation Measurements 29, 65-79.

Pagonis V. (1998) The effect of annealing atmosphere on he themoluminescence of synthetic calcite. Radiation Measurements 29, 45-52.

Péwé T.L., Berger G.W., Westgate J.A., Brown P.M. and Leavitt S.W. (1997) Eva interglaciation forest bed, unglaciated east-central Alaska. Geological Society of America, Special Paper 319, 1-56.

Roberts, R.G., Bird, M., Olley, J., Galbraith, R., Lawson, E., Laslett, G., Yoshida, H., Jones, R., Fullagar, R., Jacobsen, G. and Hua, Q. (1998) Optical and radiocarbon dating at Jinmium rock shelter in northern Australia. Nature, 393, 358-362.

Rodbell D.T., Forman S.L., Pierson J. and Lynn W.C. (1997) Stratigraphy and chronology of Mississippi Valley loess in western Tennessee. Bulletin of the Geological Society of America 109, 1134-1148.

Sakurai T. and Gartia R.K. (1997) Evidence of continuous trap distribution in the glow of a brown microcline. Journal of Applied Physics 82, 5722-5727.

Sampson C.G., Bailiff I. and Barnett S. (1997) Thermoluminescence dates from Later Stone Age pottery on surface sites in the Upper Karoo. South African Archaeological Bulletin 52, 38-42.

Sholom S.V., Haskell E.H., Hayes R.B., Chumak V.V. and Kenner G.H. (1998) Influence of crushing and additive irradiation procedures on EPR dosimetry of tooth enamel. Radiation Measurements 29, 105-111.

Sholom S.V., Haskell E.H., Hayes R.B., Chumak V.V. and Kenner G.H. (1998) Properties of light induced EPR signals in enamel and their possible interference with gamma-induced signals. Radiation Measurements 29, 113-118.

Sirovich L. (1998) First evidence of an interglacial lake of Eemian age in northeast Italy. Journal of Quaternary Science 13, 65-71.

Stokes S. (1997). Dating of desert sequences. In Arid Zone Geomorphology (editor D.S.G. Thomas) Chichester, John Wiley. 607-637.

Stokes S., Haynes G., Thomas D.S.G., Horrocks J.L., Higginson M. and Malifa M. (1998) Punctuated aridity in southern Africa during the last glacial cycle: the chronology of linear dune construction in the northeastern Kalahari. Palaeogeography, Palaeoclimatology, Palaeoecology 137, 305-322.

Stokes S. and Swinehart J.B. (1997) Middle- and late-Holocene dune reactivation in the Nebraska Sand Hills, USA. The Holocene 7, 263-272.

Stokes S. and Horrocks J. (1998). A reconnaissance survey of the linear dunes and loess plains of northwestern Nigeria: granulometry and geochronology. In Quaternary Deserts and Climatic Change (eds Alsharhan, Glennie, Whittle and Kendall). Rotterdam, Balkema. 165-174.

Stokes S., Maxwell T.A., Haynes C.V. and Horrocks J. (1998). Latest Pleistocene and Holocene sand-sheet reconstruction in the Selima Sand Sea, Eastern Sahara. In Quaternary Deserts and Climatic Change (eds Alsharhan, Glennie, Whittle and Kendall). Rotterdam, Balkema. 175-183.

Thomas D.S.G., Bateman M.D., Mehrshahi D. and O'Hara S.L. (1997) Development and environmental significance of an eolian sand ramp of last-glacial age, central Iran. Quaternary Research 48, 155-161.

Thomas D.S.G., Stokes S. and Shaw P.A. (1997) Holocene aeolian activity in the southwestern Kalahari Desert, southern Africa: significance and relationships to late-Pleistocene dune-building events. The Holocene 7, 273-281.

Thomas D.S.G., O'Connor P.W. and Stokes S. (1998). Late Quaternary aridity in the southwestern Kalahari Desert: new contributions from Optically Stimulated Luminescence (OSL) dating of aeolian deposits, northern Cape

Province, South Africa. In Quaternary Deserts and Climatic Change (eds Alsharhan, Glennie, Whittle and Kendall). Rotterdam, Balkema. 213-224.

Wende R., Nanson G.C. and Price D.M. (1997) Aeolian and fluvial evidence for Late Quaternary environmental change in the east Kimberley of Western Australia. Australian Journal of Earth Sciences 44, 519-526.

Wintle A.G. and Murray A.S. (1997) The relationship between quartz thermoluminescence, photo-transferred thermoluminescence and optically stimulated luminescence. Radiation Measurements 27, 611-624.

Wintle A.G. and Murray A.S. (1998) Towards the development of a preheat procedure for OSL dating of quartz. Radiation Measurements 29, 81-94.

Woodborne S. and Vogel J.C. (1998) Luminescence dating at Rose Cottage Cave: a progress report. South African Journal of Science 93, 476-478.

Young R.W., Bryant E.A., Price D.M., Dilek S.Y. and Wheeler D.J. (1997) Chronology of Holocene Tsunamis on the Southeastern Coast of Australia. Transactions of the Japanese Geomorphological Union 18, 1-19.

A **Special Issue of Radiation Measurements** was published at the end of 1997, as a companion volume to the Canberra conference published in the same journal the previous April.
The topic was Luminescence and ESR dating and allied research.
The guest editor was Ann Wintle, and it was issue 5/6 of volume 27, pages 625-1025.
It contained the following papers